Original Article

Volumetric assessment of solid pulmonary nodules on ultralow-dose CT: a phantom study

Matthias Eberhard[1], Daniel Stocker[1], Gianluca Milanese[2], Katharina Martini[1], Thi Dan Linh Nguyen-Kim[1], Moritz C. Wurnig[1], Thomas Frauenfelder[1], Stephan Baumueller[1]

[1]Institute of Diagnostic and Interventional Radiology, University Hospital Zurich, Zurich, Switzerland; [2]Division of Radiology, Department of Medicine and Surgery (DiMeC), University of Parma, Parma, Italy

Contributions: (I) Conception and design: S Baumüller, M Eberhard; (II) Administrative support: T Frauenfelder; (III) Provision of study materials or patients: S Baumueller; (IV) Collection and assembly of data: M Eberhard, G Milanese, K Martini; (V) Data analysis and interpretation: M Eberhard, M Wurnig, G Milanese, D Stocker; (VI) Manuscript writing: All authors; (VII) Final approval of manuscript: All authors.

Correspondence to: Matthias Eberhard, MD. Institute of Diagnostic and Interventional Radiology, University Hospital Zurich, Raemistrasse 100, 8091 Zurich, Switzerland. Email: matthias.eberhard@usz.ch.

Background: To reduce the radiation exposure from chest computed tomography (CT), ultralow-dose CT (ULDCT) protocols performed at sub-millisievert levels were previously tested for the evaluation of pulmonary nodules (PNs). The purpose of our study was to investigate the effect of ULDCT and iterative image reconstruction on volumetric measurements of solid PNs.

Methods: CT datasets of an anthropomorphic chest phantom containing solid microspheres were obtained with a third-generation dual-source CT at standard dose, 1/8th, 1/20th and 1/70th of standard dose [CT volume dose index ($CTDI_{vol}$): 0.03–2.03 mGy]. Semi-automated volumetric measurements were performed on CT datasets reconstructed with filtered back projection (FBP) and advanced modelled iterative reconstruction (ADMIRE), at strength level 3 and 5. Absolute percentage error (APE) evaluated measurement accuracy related to the effective volume. Scan repetition differences were evaluated using Bland-Altman analysis. Two-way analysis of variance (ANOVA) assessed influence of different scan parameters on APE. Proportional differences (PDs) tested the effect of dose settings and reconstruction algorithms on volumetric measurements, as compared to the standard protocol (standard dose-FBP).

Results: Bland-Altman analysis revealed small mean interscan differences of APE with narrow limits of agreement (–0.1%±4.3% to –0.3%±3.8%). Dose settings (P<0.001), reconstruction algorithms (P<0.001), nodule diameters (P<0.001) and nodule density (P=0.011) had statistically significant influence on APE. Post-hoc Bonferroni tests showed slightly higher APE when scanning with 1/70th of standard dose [mean difference: 3.4%, 95% confidence interval (CI): 2.5–4.3%; P<0.001], and for image reconstruction with ADMIRE5 (mean difference: 1.8%, 95% CI: 1.0–2.5%; P<0.001). No significant differences for scanning with 1/20th of standard dose (P=0.42), and image reconstruction with ADMIRE3 (P=0.19) were found. Scanning with 1/70th of standard dose and image reconstruction with FBP showed the widest range of PDs (–16.8% to 23.4%) compared to standard dose-FBP.

Conclusions: Our phantom study showed no significant difference between nodule volume measurements on standard dose CT ($CTDI_{vol}$: 2 mGy) and ULDCT with 1/20th of standard dose ($CTDI_{vol}$: 0.10 mGy).

Keywords: Image reconstruction; multidetector computed tomography (multidetector CT); solitary pulmonary nodule (solitary PN)

Submitted Feb 20, 2019. Accepted for publication Jul 19, 2019.
doi: 10.21037/jtd.2019.08.12
View this article at: http://dx.doi.org/10.21037/jtd.2019.08.12

Introduction

Multidetector chest computed tomography (CT) scanning represents a cornerstone for the detection of small pulmonary nodules (PNs) (1-3). The likelihood of malignancy in a PN correlates with its size and growth rate, as the vast majority of PNs represent benign lesions (4,5). Caliper measurement of nodule diameter is currently the most widely used approach to assess size and growth during follow-up (5-7). However, volumetric measurements provide superior reproducibility compared to caliper measurements and may allow a more precise calculation of volume doubling time (VDT) as the evaluation of PNs on a three-dimensional basis may reflect the morphology more precisely (6,8,9). Recently, volume measurements have been included by several guidelines for PN management strategies (10-13).

The greatest drawback of CT is related to the increasing risk of developing cancer because of radiation exposure (14), which could be particularly relevant in patients undergoing repeated scanning during follow-up of PN. Different methods to decrease radiation burden have been established, including extreme reduction of tube current and scanning with reduced tube voltage, both leading to ultralow-dose CT (ULDCT) (15-18). Iterative reconstruction algorithms received much attention in the effort to reduce radiation dose while maintaining image quality, because of their ability to provide similar noise levels at lower radiation doses, compared to standard examinations with filtered back projection (FBP) (16,17,19-22). Second generation iterative reconstruction algorithms offer a higher resolution at organ borders, and improved delineation of edges and therefore are beneficial for PN detection on ULDCT (16,17,23). In ULDCT of the chest with radiation doses comparable to chest radiographs and image reconstruction with advanced modelled iterative reconstruction (ADMIRE), sensitivity for detection of solid PN remains high (17). However, the effect of ULDCT protocols and image reconstruction with ADMIRE on reproducibility of volumetric measurements represents the major factor to be tested before the implementation of such scanning protocols in daily clinical practice. The objective of our study was to investigate whether ULDCT scanning protocols and ADMIRE algorithm have an influence on volumetric assessment of solid PN.

Methods

Anthropomorphic chest phantom

CT scans of a custom-made anthropomorphic chest phantom (serial number QSA-452; Quality Assurance in Radiology and Medicine, Moehrendorf, Germany) were obtained at different radiation doses (17,23). The phantom represents the chest of an adult male (with a lateral diameter of 30 cm and an anteroposterior diameter of 20 cm). Cork granulate was used to represent normal lung parenchyma and interstitium with an attenuation of approximately—850 Hounsfield units (HU) at 120 kVp. Resin, calcium carbonate, magnesium oxide and hydroxyapatite were used to simulate soft tissue, lung-, and bone-equivalent structures. The phantom contains 15 microspheres acting as solid PN with diameters ranging from 4 to 10 mm (attenuation of 20–80 HU at 120 kVp) as shown in *Table 1*.

CT scanning protocol

All CT datasets were acquired by using single-energy scanning protocol on a third-generation dual-source CT (SOMATOM® Force; Siemens Healthineers, Forchheim, Germany) equipped with an integrated high-resolution circuit detector (Stellar detector; Siemens Healthineers). Standard chest CT was performed at 120 kVp with 100 reference mAs using time current modulation (CareDose4D; Siemens Healthineers, Forchheim, Germany). Subsequent low-dose image acquisition was performed at a tube voltage of 100 kVp using tin filtration. For low- dose scans, tube current–time modulation was not applied to obtain three different radiation dose levels [CT volume dose index ($CTDI_{vol}$): 1/8th, 1/20th and 1/70th of the standard dose scan] as previously described (17) (*Table 2*). Further acquisition parameters for all scans were as follows: detector collimation, 192 mm × 0.6 mm; slice width, 1.5 mm; gantry rotation time, 0.25 s; pitch, 1.2; field of view, 350 mm; matrix size, 512 pixels × 512 pixels. Scans included the entire phantom with a constant scan length of 20 cm in z-axis. The phantom was scanned once with each dose setting. CT scans with all dose settings were obtained sequentially on the same day without changing the position of the phantom or the nodules within. The phantom was scanned with the same protocol (*Table 2*) on three different days, afterwards called day 1, day 2 and day 3. On day 3, the phantom was scanned in prone position.

Data reconstruction

Acquired CT scans were reconstructed with two reconstruction algorithms, namely FBP and ADMIRE (Siemens Healthineers, Forchheim, Germany), the latter at

Table 1 Nodule characteristics

Nodule characteristics	Nodule diameter (mm)				Total
	4	6	8	10	
HU					
20	2	1	1	1	5
50	1	1	1	1	4
80	1	2	1	2	6
Total	4	4	3	4	15

HU, Hounsfield unit.

Table 2 Scan protocol

Dose settings	Scanning protocol		Day 1		Day 2		Day 3	
	kVp	mAs ref	mAs eff	$CTDI_{vol}$ (mGy)	mAs eff	$CTDI_{vol}$ (mGy)	mAs eff	$CTDI_{vol}$ (mGy)
Standard	120	100	36	2.03	29	1.99	30	2.03
1/8	100 Sn	–	75	0.26	75	0.26	75	0.26
1/20	100 Sn	–	30	0.10	30	0.10	30	0.10
1/70	100 Sn	–	10	0.03	10	0.03	10	0.03

Standard dose scans were performed, applying tube current modulation. Low- and ultralow-dose scans were performed without tube current modulation. There, the effective tube-current time product was adjusted in order to achieve 1/8, 1/20 and 1/70 of $CTDI_{vol}$ of our standard dose scan. $CTDI_{vol}$, computed tomography dose index; eff, effective; ref, reference; Sn, tin filtration.

strength levels 3 and 5 as previously described (17). *Figure 1* shows representative images of a solid nodule (10 mm) obtained with different dose levels and different image reconstruction algorithms.

Images were reconstructed with the following parameters: slice thickness, 1.5 mm; increment, 1 mm; kernel, sharp tissue convolution kernel (B64 for FBP and I64 for ADMIRE).

Semi-automated nodule volumetry

One observer (G. M.) performed semi-automated volumetric measurements using a commercially available software package (MM Oncology, syngo.via, Siemens Healthineers, Forchheim, Germany) in datasets with different combinations of dose settings and image reconstruction algorithms of day 1, day 2, and day 3. Additional two observers (D. S. and T. N.) performed semi-automated volumetric measurements in all scans of day 1. Observers had to place a seed point on the nodule to initiate semi-automatic nodule segmentation. Subsequently observers could evaluate segmentation and adjust the volume manually. No observer had a priori knowledge of phantom nodule sizes.

Statistical analysis

Lin's concordance correlation coefficient (LCCC) tested interobserver reproducibility between two observers, comparing volumetric measurements performed by observer 1, observer 2, and observer 3 on scans of day 1. LCCC also tested interscan reproducibility of volume measurements of observer 1 on scans of day 1, day 2, and day 3. LCCC assesses how close measurements are about the line of best fit and how far that line is from the 45° line through the origin (24). According to the thresholds proposed by McBride, values >0.99 are defined as excellent agreement (25). Bland-Altman analysis was applied to evaluate differences of absolute percentage errors (APE) of scans on day 1, day 2, and day 3.

As we found excellent interobserver agreement, further analyses were performed only with measurements of observer 1.

To compare accuracy of volumetric measurements

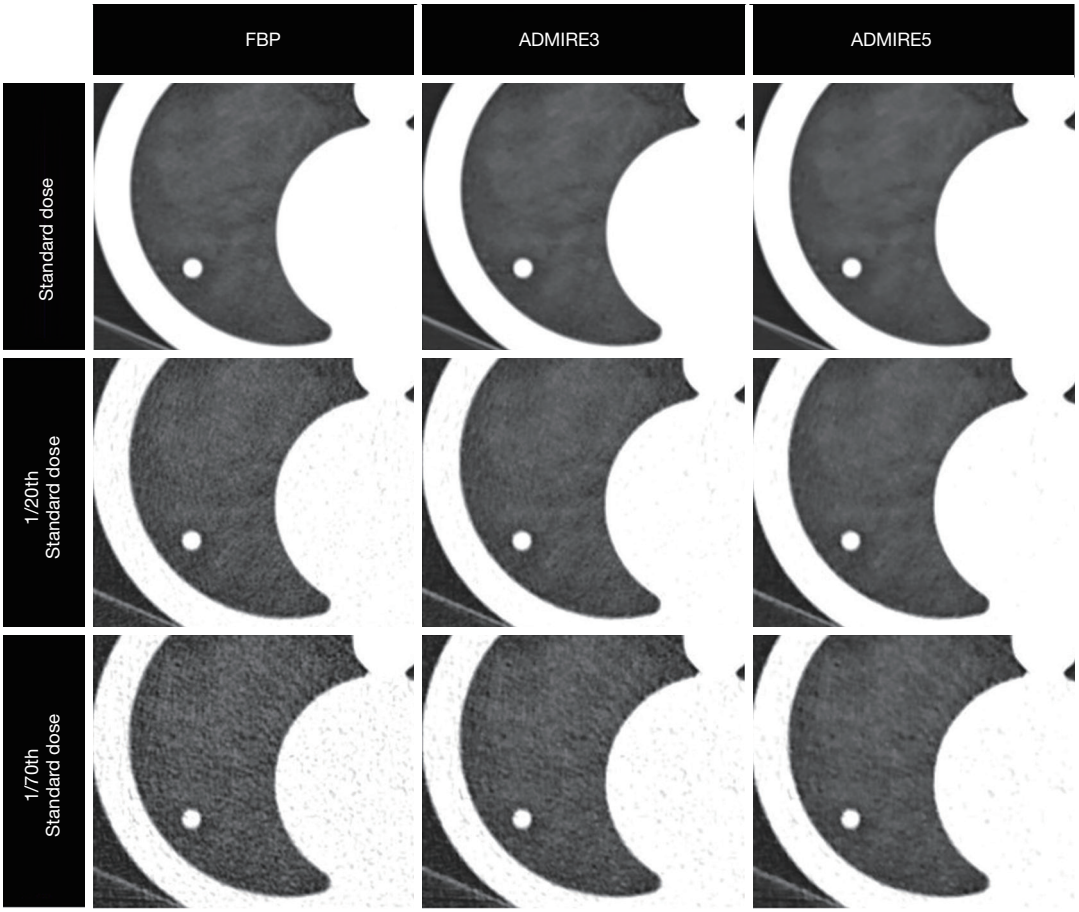

Figure 1 Representative images of a solid nodule (10 mm) obtained with different dose levels (standard dose, $CTDI_{vol}$: 2.03 mGy; 1/20th of standard dose, $CTDI_{vol}$: 0.10 mGy; 1/70th of standard dose, $CTDI_{vol}$: 0.03 mGy) and different image reconstruction algorithms (FBP, ADMIRE at strength level 3, ADMIRE at strength level 5). $CTDI_{vol}$, computed tomography volume dose index; ADMIRE, advanced modelled iterative reconstruction; FBP, filtered back projection.

between reconstruction protocols we calculated the APE of measurements. Measured nodule volume (V_m) and calculated nodule volume (V_c) were used to calculate percentage errors. V_c was given by the constructional drawing. APE was calculated as $100 \times (|(V_m - V_c)/V_c|)$ to indicate error margin and accuracy of nodule volumetry.

To assess differences of reconstruction algorithms in comparison to our standard protocol (standard dose; image reconstruction with FBP, afterwards called SD-FBP) we applied the proportional difference (PD) metric described by Bland and Altman (26). The PD metric was previously recommended for the comparison of PN volume with different reconstruction techniques (27). This metric describes the PD of each nodule volume at each reconstruction protocol (V_{prot}) in comparison to the volume of the same nodule measured at SD-FBP on the same scan ($V_{SD\text{-}FBP}$) and is calculated as follows: $100 \times (V_{prot} - V_{SD\text{-}FBP})/(V_{prot} + V_{SD\text{-}FBP})$.

APE and PD are expressed as means ± standard deviation. One-way analysis of variance (ANOVA) was applied to assess differences of APE between scans of day 1–day 3. To assess the influence of dose settings and image reconstruction algorithms on APE we performed a two-way ANOVA to compensate for the influence of co-variates (nodule diameters, nodule density, scan acquisition day). Afterwards post-hoc Bonferonni test was applied. Mean differences assessed with post-hoc Bonferroni tests are expressed as mean and 95% confidence interval (95% CI).

P<0.05 was considered statistically significant. Statistical analyses were conducted using commercially available

Table 3 Nodule volume measurements: mean nodule volume and APE

Nodule diameter (volume)	Dose setting	Reconstruction algorithm		
		FBP, mm^3 (%)	ADMIRE3, mm^3 (%)	ADMIRE5, mm^3 (%)
4 mm (33.5 mm^3)	Standard dose	35±1 (3.5)	31±1 (6.3)	29±1 (12.7)
	1/8 dose	35±2 (4.5)	33±1 (4.0)	32±1 (6.5)
	1/20 dose	34±3 (6.2)	33±2 (6.5)	31±2 (7.7)
	1/70 dose	37±4 (11.7)	33±3 (7.0)	32±4 (9.0)
6 mm (113.1 mm^3)	Standard dose	109±2 (3.8)	105±2 (7.0)	103±1 (8.9)
	1/8 dose	105±2 (7.2)	106±2 (6.6)	105±2 (7.3)
	1/20 dose	104±3 (7.8)	103±2 (8.6)	103±3 (9.1)
	1/70 dose	97±4 (14.5)	98±3 (13.4)	101±4 (10.9)
8 mm (268.1 mm^3)	Standard dose	268±3 (0.7)	264±6 (2.5)	258±3 (3.8)
	1/8 dose	265±5 (1.8)	263±5 (2.5)	259±4 (3.5)
	1/20 dose	267±5 (1.4)	261±3 (2.6)	258±4 (3.6)
	1/70 dose	258±7 (4.0)	253±6 (5.6)	250±7 (6.7)
10 mm (523.6 mm^3)	Standard dose	511±8 (2.6)	503±7 (4.0)	499±6 (4.7)
	1/8 dose	506±6 (3.4)	502±7 (4.2)	498±6 (4.9)
	1/20 dose	504±7 (3.8)	499±7 (4.8)	495±7 (5.5)
	1/70 dose	494±6 (5.7)	489±6 (6.6)	490±6 (6.4)

Mean volume (mm^3) and mean absolute percentage error (in brackets) are shown for each combination of nodule diameter, phantom size, reconstruction algorithm and dose setting. APE, absolute percentage error; ADMIRE, advanced modeled iterative reconstruction; FBP, filtered back projection.

software (IBM SPSS®, version 25.0, IBM Corp, Armonk, NY, USA).

Results

Interobserver and interscan variability

Semi-automatic volumetric measurements were successfully performed for every nodule at each radiation dose setting and reconstruction algorithm by all observers, resulting in 540 measurements of observer 1 and 180 measurements of observer 2 and 3, respectively.

Interobserver agreement was excellent between observer 1 and 2 (LCCC: 1.0, 95% CI: 1.00–1.00), between observer 1 and 3 (LCCC: 1.0, 95% CI: 1.00–1.00) and between observer 2 and 3 (LCCC: 1.0, 95% CI: 1.00–1.00).

Assessment of interscan reproducibility of observer 1 showed excellent agreement of measurements between scans on day 1 and day 2, (LCCC: 1.0, 95% CI: 0.99–1.00) between scans on day 1 and day 3 (LCCC: 1.0, 95% CI: 1.00–1.00) and between scans on day 2 and day 3 (LCCC: 1.0, 95% CI: 0.99–1.00).

Bland-Altman analysis revealed small mean differences of APE with narrow limits of agreement between measurements of day 1 and day 2 (mean difference: –0.1%±4.3%), day 1 and day 3 (–0.3%±3.8%), as well as day 2 and day 3 (–0.2%±4.2%).

Nodule volume and measurement accuracy

Mean nodule volumes according to nodule diameter, reconstruction algorithms and dose settings are displayed in *Table 3*.

APEs were comparable between scans. Mean APE was 6.0%±4.2% for scans on day 1, 6.1%±4.3% for scans on day 2 and 6.3%±3.9% for scans on day 3. One-way ANOVA did not show a significant difference of APE between scans of day 1, day 2, and day 3 with P=0.76.

When comparing APE between reconstruction protocols

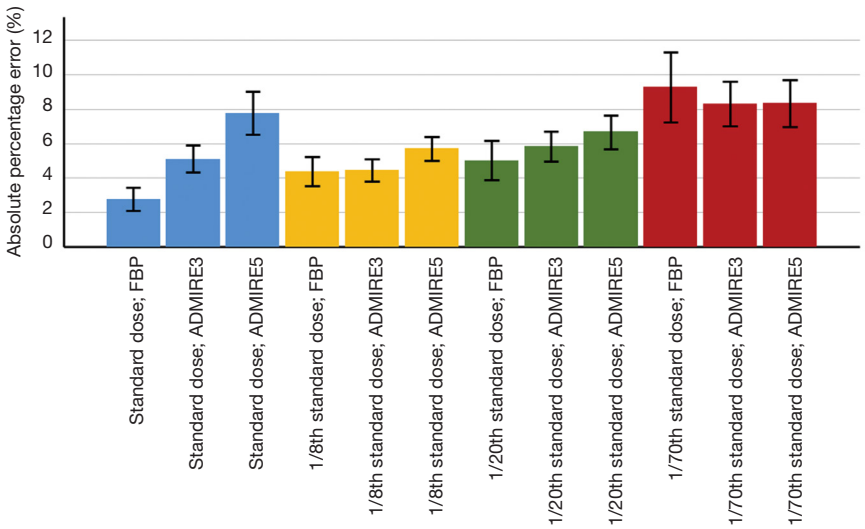

Figure 2 Mean APE (± standard deviation) for each combination of reconstruction algorithms and dose settings. Lowest mean APE was found for our standard protocol (standard dose scan; image reconstruction with FBP). APE, absolute percentage error; FBP, filtered back projection; ADMIRE, advanced modelled iterative reconstruction.

including all size of nodules, *Figure 2* shows that mean APE was lowest for standard dose scans with image reconstruction with FBP (2.8%±2.2%) and highest for ULDCT with 1/70th of standard dose scans and image reconstruction with FBP with 9.3%±6.7%.

Effects of nodule characteristics and CT parameters on APE

Dose settings (P<0.001), image reconstruction algorithms (P<0.001), nodule diameters (P<0.001) and nodule densities (P=0.011) had statistically significant influence on APE, whereas measurement differences between scans of day 1–3 had no significant influence (P=0.430). Post-hoc Bonferroni test showed that only ULDCT with 1/70th of standard dose had a significant effect on APE with an estimated mean difference of 3.4% with a 95% CI of 2.5–4.3% (P<0.001) compared to scanning with standard dose. There was no significant difference of scanning with 1/8th (estimated mean difference: –0.4%; 95% CI: –1.3% to 0.5%; P=1.000) and 1/20th (estimated mean difference: 0.6%; 95% CI: –0.3% to 1.5%; P=0.420) of standard dose compared to scanning with standard dose. Furthermore, post-hoc Bonferroni test showed a significant higher APE when ADMIRE at strength level 5 was applied (estimated mean difference: 1.8%; 95% CI: 1.0–2.5%; P<0.001). No significant difference of APE was found between FBP and ADMIRE at strength level 3 (estimated mean difference: 0.6%; 95% CI: –0.2% to 1.5%; P=0.190).

Comparison of PDs between protocols

Comparison of PDs of each combination of dose setting and image reconstruction algorithm with SD-FBP showed a tendency of underestimation of nodule volumes, notably in 4 mm nodules, when scanning with low-dose and by applying ADMIRE (*Figure 3*, *Table 4*).

Range of PDs was higher in ULDCT with 1/70th of standard dose. Widest range of PDs (in comparison to SD-FBP) was found for scanning with 1/70th of standard dose and image reconstruction with FBP with 40.2% (range, –16.8% to 23.4%; *Figure 3*).

Furthermore, the ranges of PDs of each protocol were highest for 4 mm nodules (coloured in blue in *Figure 3*). In comparison to SD-FBP, maximum volume over- and underestimations for 4 mm nodules were –29.5% (ULDCT with 1/70th of standard dose and ADMIRE at strength level 5) and 23.4% (ULDCT with 1/70th of standard dose and FBP), respectively. For nodules ≥6 mm, maximum volume over- and underestimations were –16.8% (ULDCT at 1/70th of standard dose and FBP) and 3.3% (standard dose and ADMIRE at strength level 3), respectively. Mean PD and range of PDs of nodule volumes according to nodule diameter for each set of dose setting and image

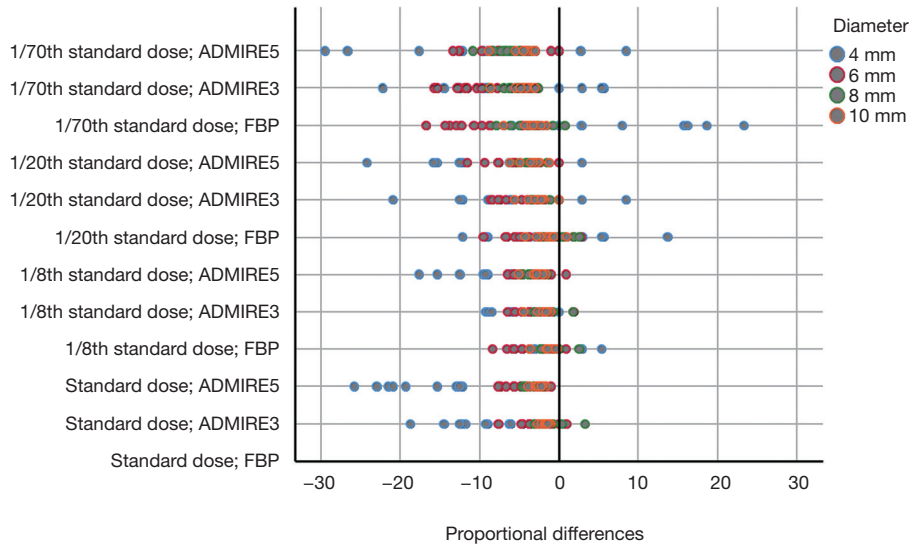

Figure 3 PDs for each combination of reconstruction algorithms and dose settings in comparison to our standard protocol (standard dose, FBP) showed a tendency for underestimation of nodule volumes, notably in 4 mm nodules (coloured in blue), when scanning with low-dose and by applying iterative image reconstruction. FBP, filtered back projection; ADMIRE, advanced modelled iterative reconstruction; PD, proportional difference.

reconstruction algorithm in comparison to SD-FBP are shown in *Table 4*.

Discussion

Our phantom study showed that there are no significant differences of nodule volume measurements on ULDCT with 1/20th of standard dose ($CTDI_{vol}$: 0.1 mGy) compared to volume measurements on standard dose protocols ($CTDI_{vol}$: 2.0 mGy). ULDCT at 1/70th of standard dose and image reconstruction with ADMIRE at strength level 5 led to slightly but statistically significant reduced measurement accuracy.

PN size and growth rate are the main predictors of malignancy (4,7,11,28). Recommendations for PN management focus on follow-up CTs for nodules at intermediate risk (4,10,11,29). Several lung cancer screening trials incorporated PN volume assessment within their protocols (12,13,30). Furthermore, the most recent guidelines of the British Thoracic Society (BTS) and the Fleischner Society for the management of PNs also recognized the role of volumetry to aid nodule measurement and management (10,11). For follow-up of PN and VDT assessment, it is crucial to preserve comparability of volume measurements as the influence of dose settings and image reconstruction technique may influence patient treatment.

The high intrinsic contrast between air and pulmonary structures is beneficial for radiation dose reduction in chest CT. Several studies concluded that nodule measurement accuracy is not affected by substantial reduction of radiation dose (6,31,32). Previously it was reported that PN volumetry can be accurately performed *in vivo* at a CTDIvol down to 1.0 mGy (33). However, excessive dose reduction may degrade nodule boundary definition and therefore affect performance of PN volumetry. Iterative image reconstruction may affect nodule volumetry due to changes in nodule density and nodule texture (34). For solid nodules, den Harder *et al.* showed no significant differences between *in vivo* volumetric measurements for FBP and iterative reconstruction (IR), although IR resulted in smaller volume measurements with a maximum difference of –11% compared to FBP (33). Doo *et al.* showed slightly more accurate volumetric measurements of solid nodules in a phantom model for FBP datasets as compared to IR; however, this difference did not reach statistical significance (34). Our findings suggest that volumetry of PN could be performed at dose levels down to 0.10 mGy without significant reduction of measurement accuracy. Thus, volume measurements of standard dose chest CTs and ULDCTs may be comparable in follow-up examinations, as only the ULDCT scans with 1/70th of standard dose significantly increased APE. The slightly

Table 4 PDs of nodule volume according to nodule diameter for each set of dose setting and image reconstruction algorithm in comparison to the standard protocol (standard dose scan, image reconstruction with FBP)

Dose setting	Reconstruction algorithm	Nodule diameter 4 mm		Nodule diameter 6 mm		Nodule diameter 8 mm		Nodule diameter 10 mm	
		Mean PD (%)	Range PD (%)	Mean PD (%)	Range PD (%)	Mean PD (%)	Range PD (%)	Mean PD (%)	Range PD (%)
Standard dose	ADMIRE3	–9.6	–18.8 to –3.0	–3.4	–7.6 to 1.0	–1.3	–3.0 to 3.3	–1.7	–2.7 to –1.0
	ADMIRE5	–16.8	–25.8 to –12.1	–5.4	–7.7 to –1.9	–3.7	–4.6 to –3.0	–2.4	–3.8 to –1.6
1/8th standard dose	FBP	–0.1	–5.9 to 5.4	–3.6	–8.4 to 0.9	–0.8	–2.3 to 2.6	–1.1	–3.6 to –0.2
	ADMIRE3	–5.5	–9.2 to 0.0	–3.0	–6.5 to 1.8	–1.7	–3.0 to 1.8	–1.9	–4.4 to –1.0
	ADMIRE5	–9.1	–17.7 to –2.8	–3.7	–6.5 to 0.9	–3.4	–5.0 to –1.5	–2.7	–5.0 to –1.6
1/20th standard dose	FBP	–1.9	–12.1 to 13.7	–4.3	–9.52 to 2.8	–0.1	–1.9 to 2.6	–1.5	–4.2 to 1.0
	ADMIRE3	–6.1	–20.9 to 8.5	–5.2	–8.5 to 0.0	–2.5	–3.4 to –1.1	–2.5	–5.6 to 0.0
	ADMIRE5	–10.2	–24.2 to 2.9	–5.7	–11.5 to 0.0	–3.5	–5.0 to –1.5	–3.2	–6.2 to –1.2
1/70th standard dose	FBP	6.3	–6.1 to 23.4	–11.8	–16.8 to –4.7	–3.6	–7.9 to 0.7	–3.5	–7.0 to –1.6
	ADMIRE3	–5.7	–22.2 to 5.7	–10.5	–15.7 to –2.9	–5.6	–8.7 to –2.6	–4.5	–8.6 to –3.0
	ADMIRE5	–8.8	–29.5 to 8.5	–7.8	–13.3 to 0.0	–6.7	–10.8 to –3.8	–4.2	–8.8 to –3.0

ADMIRE, advanced modelled iterative reconstruction; FBP, filtered back projection, PD, proportional difference.

reduced measurement accuracy may lead to a wider range of PDs of ULDCT with 1/70th of standard dose (0.03 mGy), compared to SD-FBP. Previously, it was also shown that the sensitivity for the detection of solid PNs remains high with ULDCT and iterative image reconstruction down to a CTDIvol of 0.1 mGy, whereas lower doses reduced the sensitivity for nodule detection (16,17). Interestingly, application of ADMIRE led to higher APE in scans with standard dose as well as scans with 1/8th and 1/20th of standard dose but decreased APE in ULDCT scans with 1/70th of standard dose. This effect may partly be explained by variation of nodule density and nodule texture as well as improved delineation of edges using second generation iterative reconstruction algorithms compared to image reconstruction with FBP (16,17,23,35).

Similar to our study, previous studies reported increasing volume measurement error with decreasing nodule size (36,37). Notably, volume underestimation is more common in smaller nodules (38), and measurement variability increases with decreasing nodule diameter (39). In comparison to SD-FBP, we found underestimation of nodule volume for ultralow-dose scans and image reconstruction with ADMIRE. In nodules ≥6 mm we found a maximum PD of –16.8% when ultralow-dose scanning was performed. That means, when comparing measurements between a baseline SD-FBP CT and a follow-up low-dose CT or ULDCT with application of ADMIRE, nodule growth may be underestimated, and VDT calculation may be affected. Additionally, nodule volume underestimation may lead to a change of patient management recommendations, for example, for nodule volumes near the cut-off of 80 mm^3, proposed by the BTS for follow-up imaging. In these cases, nodule volume underestimation at ULDCT may lead to the decision not to perform follow-up imaging, whereas volume measurements of the same nodules at SD-FBP may lead to the decision to perform follow-up CT (10).

This study has several limitations. First, we used an anthropomorphic chest phantom simulating a male adult which contains synthetic nodules. We did not assess differences in phantoms with different sizes (to simulate differences in body mass index). In addition, influence of cardiac motion and breathing could not be simulated. However, using an anthropomorphic chest phantom allows the standardization of measurements between scans with different dose settings without ethical issues of radiation exposure to patients. Second, our study includes only solid nodules as our software did not allow for volumetric assessment of subsolid nodules, which means that we cannot generalize our results to subsolid nodules. However, the execution of volumetric measurements of subsolid nodules is still under investigation (5). Third, our chest phantom only includes spheric nodules without complex borders

and the phantom does not simulate nodules near the mediastinum or with pleural attachment. Fourth, only one semi-automated software package for PN volumetry was applied and only one CT scanner with its vendor-specific reconstruction algorithm was used. Therefore, our results may have been different when using different software or a different CT scanner as it is known that different software packages can yield substantially different results for volumetric assessment of PN (40).

Conclusions

Our phantom study showed no significant differences of nodule volume measurements between standard dose and ULDCT with 1/20th of standard dose (0.10 mGy). Volume measurements on ULDCT may therefore be comparable with standard dose measurements in follow-up examinations. Further studies should assess whether our results can be confirmed in a human cohort.

Acknowledgments

This study was funded by Swiss Lung Association Zurich "Lungenliga Zürich".

Footnote

Conflicts of Interest: The authors have no conflicts of interest to declare.

Ethical Statement: The authors are accountable for all aspects of the work in ensuring that questions related to the accuracy or integrity of any part of the work are appropriately investigated and resolved.

References

1. Fischbach F, Knollmann F, Griesshaber V, et al. Detection of pulmonary nodules by multislice computed tomography: improved detection rate with reduced slice thickness. Eur Radiol 2003;13:2378-83.
2. Gould MK, Tang T, Liu IL, et al. Recent trends in the identification of incidental pulmonary nodules. Am J Respir Crit Care Med 2015;192:1208-14.
3. Qian F, Yang W, Chen Q, et al. Screening for early stage lung cancer and its correlation with lung nodule detection. J Thorac Dis 2018;10:S846-59.
4. Horeweg N, van Rosmalen J, Heuvelmans MA, et al. Lung cancer probability in patients with CT-detected pulmonary nodules: a prespecified analysis of data from the NELSON trial of low-dose CT screening. Lancet Oncol 2014;15:1332-41.
5. Bankier AA, MacMahon H, Goo JM, et al. Recommendations for measuring pulmonary nodules at CT: a statement from the Fleischner Society. Radiology 2017;285:584-600.
6. Devaraj A, van Ginneken B, Nair A, et al. Use of volumetry for lung nodule management: theory and practice. Radiology 2017;284:630-44.
7. Li J, Xia T, Yang X, et al. Malignant solitary pulmonary nodules: assessment of mass growth rate and doubling time at follow-up CT. J Thorac Dis 2018;10:S797-S806.
8. Yankelevitz DF, Reeves AP, Kostis WJ, et al. Small pulmonary nodules: volumetrically determined growth rates based on CT evaluation. Radiology 2000;217:251-6.
9. Jennings SG, Winer-Muram HT, Tarver RD, et al. Lung tumor growth: assessment with CT--comparison of diameter and cross-sectional area with volume measurements. Radiology 2004;231:866-71.
10. Callister ME, Baldwin DR, Akram AR, et al. British Thoracic Society guidelines for the investigation and management of pulmonary nodules. Thorax 2015;70 Suppl 2:ii1-ii54.
11. MacMahon H, Naidich DP, Goo JM, et al. Guidelines for management of incidental pulmonary nodules detected on CT images: from the Fleischner Society 2017. Radiology 2017;284:228-43.
12. Field JK, Duffy SW, Baldwin DR, et al. UK lung cancer RCT pilot screening trial: baseline findings from the screening arm provide evidence for the potential implementation of lung cancer screening. Thorax 2016;71:161-70.
13. van Klaveren RJ, Oudkerk M, Prokop M, et al. Management of lung nodules detected by volume CT scanning. N Engl J Med 2009;361:2221-9.
14. Brenner DJ, Hall EJ. Computed tomography—an increasing source of radiation exposure. N Engl J Med 2007;357:2277-84.
15. Bankier AA, Tack D. Dose reduction strategies for thoracic multidetector computed tomography: background, current issues, and recommendations. J Thorac Imaging 2010;25:278-88.
16. Zhang M, Qi W, Sun Y, et al. Screening for lung cancer using sub-millisievert chest CT with iterative reconstruction algorithm: image quality and nodule detectability. Br J Radiol 2018;91:20170658.

17. Martini K, Higashigaito K, Barth BK, et al. Ultralow-dose CT with tin filtration for detection of solid and sub solid pulmonary nodules: a phantom study. Br J Radiol 2015;88:20150389.
18. Padole A, Digumarthy S, Flores E, et al. Assessment of chest CT at CTDIvol less than 1 mGy with iterative reconstruction techniques. Br J Radiol 2017;90:20160625.
19. Singh S, Kalra MK, Gilman MD, et al. Adaptive statistical iterative reconstruction technique for radiation dose reduction in chest CT: a pilot study. Radiology 2011;259:565-73.
20. Prakash P, Kalra MK, Ackman JB, et al. Diffuse lung disease: CT of the chest with adaptive statistical iterative reconstruction technique. Radiology 2010;256:261-9.
21. Baumueller S, Winklehner A, Karlo C, et al. Low-dose CT of the lung: potential value of iterative reconstructions. Eur Radiol 2012;22:2597-606.
22. Deák Z, Maertz F, Meurer F, et al. Submillisievert computed tomography of the chest using model-based iterative algorithm: optimization of tube voltage with regard to patient size. J Comput Assist Tomogr 2017;41:254-62.
23. Gordic S, Morsbach F, Schmidt B, et al. Ultralow-dose chest computed tomography for pulmonary nodule detection: first performance evaluation of single energy scanning with spectral shaping. Invest Radiol 2014;49:465-73.
24. Lin LI. A concordance correlation coefficient to evaluate reproducibility. Biometrics 1989;45:255-68.
25. Willemink MJ, Borstlap J, Takx RA, et al. The effects of computed tomography with iterative reconstruction on solid pulmonary nodule volume quantification. PLoS One 2013;8:e58053.
26. Bland JM, Altman DG. Measuring agreement in method comparison studies. Stat Methods Med Res 1999;8:135-60.
27. Obuchowski NA, Reeves AP, Huang EP, et al. Quantitative imaging biomarkers: a review of statistical methods for computer algorithm comparisons. Stat Methods Med Res 2015;24:68-106.
28. Suh JH, Park JK, Moon Y. Prognostic prediction of clinical stage IA lung cancer presenting as a pure solid nodule. J Thorac Dis 2018;10:3005-15.
29. Ito M, Miyata Y, Okada M. Management pathways for solitary pulmonary nodules. J Thorac Dis 2018;10:S860-6.
30. Saghir Z, Dirksen A, Ashraf H, et al. CT screening for lung cancer brings forward early disease. The randomised Danish Lung Cancer Screening Trial: status after five annual screening rounds with low-dose CT. Thorax 2012;67:296-301.
31. Das M, Ley-Zaporozhan J, Gietema HA, et al. Accuracy of automated volumetry of pulmonary nodules across different multislice CT scanners. Eur Radiol 2007;17:1979-84.
32. Nair A, Baldwin DR, Field JK, et al. Measurement methods and algorithms for the management of solid nodules. J Thorac Imaging 2012;27:230-9.
33. den Harder AM, Willemink MJ, van Hamersvelt RW, et al. Pulmonary nodule volumetry at different low computed tomography radiation dose levels with hybrid and model-based iterative reconstruction: a within patient analysis. J Comput Assist Tomogr 2016;40:578-83.
34. Doo KW, Kang EY, Yong HS, et al. Accuracy of lung nodule volumetry in low-dose CT with iterative reconstruction: an anthropomorphic thoracic phantom study. Br J Radiol 2014;87:20130644.
35. Lo P, Young S, Kim HJ, et al. Variability in CT lung-nodule quantification: Effects of dose reduction and reconstruction methods on density and texture based features. Med Phys 2016;43:4854.
36. Goo JM, Tongdee T, Tongdee R, et al. Volumetric measurement of synthetic lung nodules with multi-detector row CT: effect of various image reconstruction parameters and segmentation thresholds on measurement accuracy. Radiology 2005;235:850-6.
37. Xie X, Willemink MJ, de Jong PA, et al. Small irregular pulmonary nodules in low-dose CT: observer detection sensitivity and volumetry accuracy. AJR Am J Roentgenol 2014;202:W202-9.
38. Willemink MJ, Leiner T, Budde RP, et al. Systematic error in lung nodule volumetry: effect of iterative reconstruction versus filtered back projection at different CT parameters. AJR Am J Roentgenol 2012;199:1241-6.
39. Liang M, Yip R, Tang W, et al. Variation in screening CT-detected nodule volumetry as a function of size. AJR Am J Roentgenol 2017;209:304-8.
40. Kim H, Park CM, Lee SM, et al. A comparison of two commercial volumetry software programs in the analysis of pulmonary ground-glass nodules: segmentation capability and measurement accuracy. Korean J Radiol 2013;14:683-91.

Cite this article as: Eberhard M, Stocker D, Milanese G, Martini K, Nguyen-Kim TDL, Wurnig MC, Frauenfelder T, Baumueller S. Volumetric assessment of solid pulmonary nodules on ultralow-dose CT: a phantom study. J Thorac Dis 2019;11(8):3515-3524. doi: 10.21037/jtd.2019.08.12

